# Membrane and Tension Structures

Realistic modeling of tensioned fabric structures
*Julio B. PARGANA, David LLOYD SMITH, Bassam A. IZZUDDIN* (Imperial College London)*

Vaccumatics: Vacuumatically prestressed (adaptable) structures
*Frank HUIJBEN*, Frans van HERWIJNEN (Eindhoven University of Technology)*

Wrinkling evaluation of membrane structures
*Lu GUO (Cybernet Systems Co.)*

Wrinkling of stretched elastic films via bifurcation
*Ron-Bin CHENG*, Tim HEALEY (Cornell University)*

A comparison of four flattening methods for tensioned fabric structures
*Slade GELLIN (Buffalo State College)*

On the calculation of elastic systems having blocks and sagging cables
*Vadym GORDEIEV*, Oleksandr OGLOBLYA, Maryna SHYMANOVSKA (V. Shimanovsky UkrRDIsteelconstruction)*

For multiple-author papers:
Contact author designated by *
Presenting author designated by underscore

Proceedings of the 6th International Conference on
Computation of Shell and Spatial Structures
IASS-IACM 2008: "Spanning Nano to Mega"
28-31 May 2008, Cornell University, Ithaca, NY, USA
John F. ABEL and J. Robert COOKE (eds.)

# Realistic modelling of tensioned fabric structures

Julio B. PARGANA, David LLOYD SMITH, Bassam A. IZZUDDIN*

*Imperial College London
Department of Civil and Environmental Engineering,
Imperial College London, London, SW7 2AZ. UK
Email: b.izzuddin@imperial.ac.uk

## Abstract

In this paper, the main features of an analysis tool developed for the realistic modelling of Tensioned Fabric Structures (TFS) are presented. It is considered that the tool allows for the realistic modelling of TFS, as high levels of accuracy and reliability have been attained for the individual components that make up the analysis tool. The basic components are: a sliding cable element, a membrane finite element and a material model for plain-weave coated fabrics. These components have been integrated into ADAPTIC, an advanced nonlinear structural analysis program, allowing the behaviour and design of real TFS to be studied closely. Through case studies, deficiencies in traditional design procedures have been identified, which may ultimately result in compromised design, as these procedures are founded on unrealistic overly simplistic assumptions. One such simplification relates to ignoring that fabric patterns are flat in there unstressed state, which presents a conflict with the manufacturing process of fabrics. It is contended that the use of more realistic modelling tools, such as the one proposed in this paper, overcomes the indentified deficiencies, leading to better designs and control over the construction of real TFS.

## 1. Introduction

Tensioned Fabric Structures (TFS) are unique structures that require special-purpose procedures for their analysis and design. TFS exhibit nonlinear behaviour due to both geometric and material effects, and both must be captured for realistic modelling. Geometric nonlinearities arise as large displacements and significant tensile stress-fields are necessary to equilibrate live loads. Moreover, large displacements are inevitably involved in moving from an initial guessed configuration to an equilibrium configuration, necessitating the use of geometrically nonlinear analysis techniques. The material response is also highly nonlinear, which is attributed to the combined effects of numerous deformation mechanisms that fabrics exhibit when subjected to planar stresses. These deformation mechanisms include crimp interchange, yarn extension, yarn crushing and coating deformations (Freeston *et al.* [3]).

The design procedure adopted for this work, known as the integrated design procedure, commences from fabric patterns that are flat in their unstressed state, which is an essential requirement for the realistic modelling and design of TFS. The principal ingredients of such a procedure include accurate and reliable finite elements which are based on realistic and validated material models. This procedure involves the nonlinear analysis of TFS starting from cutting patterns flat in their unstressed state, and the iterative adjustment of these patterns along with the cable lengths until the various design objectives are met. The integrated design procedure, illustrated in Figure 1, was first formally suggested by Abel *et al.* [1] and further elaborated by Phelan and Haber [8].

This paper presents an advanced analysis capability that can be used as for the realistic modelling of TFS as part of an integrated design procedure. Case studies are also provided, which identify deficiencies in current practice for the design of TFS, highlighting the need for more realistic modelling of such structures.

## 2. Cable and Membrane Elements

Geometrically nonlinear cable and membrane finite elements have been developed (Pargana [6]) and integrated into ADAPTIC (Izzuddin [4]). The cable element allows for sliding, which is necessary for modelling cables inside sleeves, achieved through the use of an Eulerian sliding freedom in addition to the three translational freedoms at each of the three element nodes. This element employs quadratic displacement fields and utilises the Green strain-displacement relationship for modelling the influence of large displacement. The membrane element is 6-noded triangular, thus allowing quadratic displacement fields; it is therefore compatible with the sliding cable element. The membrane element is flat in the unstrained state, as required for realistic modelling of TFS, and also utilises the Green strain-displacement relationship. ADAPTIC (Izzuddin [4]) also has beam-column and rigid link elements which may be combined with the developed membrane and cable elements.

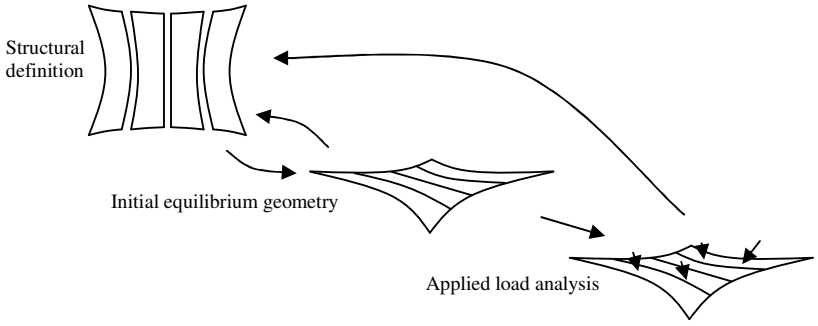


Figure 1: Integrated design procedure in diagrammatic form (Phelan and Haber [7])

## 3. Fabric Material Model

Fabrics used in the construction of TFS exhibit i) marked differences in the response of the warp and weft directions, ii) gross nonlinearities in the response, and iii) a permanent set after the first application of stress. Their response is also greatly influenced by stress ratio (Bradshaw [2]). These features are attributed to the major deformation mechanisms that prevail when fabrics are subjected to plane stress, including crimp interchange, yarn and coating extension, yarn crushing and friction.

The material model developed authentically captures the above major deformation mechanisms, consisting of i) a series of nonlinear elements that run along the length of the yarn, ii) nonlinear crushing elements, iii) rigid links, and iv) an isotropic plate to model the coating, as shown in Figure 2. The elements only offer resistance to axial forces and not to bending, those elements that run along the length of the yarn are constrained to adopt quadratic profiles, which closely resemble the true yarn profile. The model is formulated using unit cell analysis, where the unit cell is subjected to a constant strain-field and the characteristic mechanical response of the material is obtained using an energy approach (Pargana *et al*. [7]).

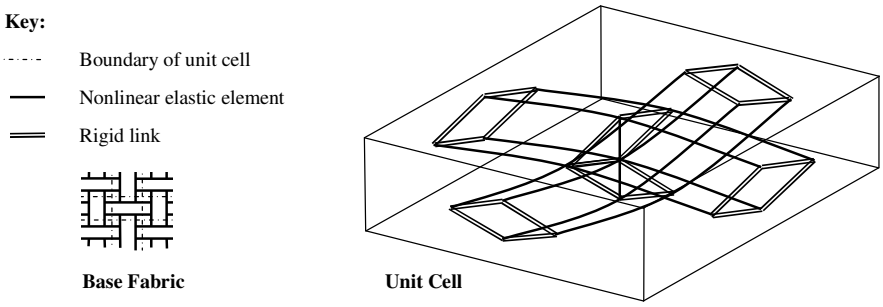


Figure 2: Material model

The material model is calibrated against experimental test data for an example of plain-weave PTFE coated glass-fibre fabric given by Kato *et al.* [5]. The achieved results for the (1:1) stress ratio are shown in Figure 3, where good comparison is achieved between the test and model results. Equally good results have been obtained for the (2:1), (1:2), (1.5:1) and (1:1.5) stress ratios, demonstrating that the model attains high levels of accuracy, reliability and robustness for the complete range of stress ratios that well designed structures are normally subjected to. Although the model has only been calibrated for one set of test data it could be successfully calibrated for other examples of fabric. This is because the model is based on authentically capturing the dominant deformation mechanisms which are the same for other examples of plain-weave coated fabric.

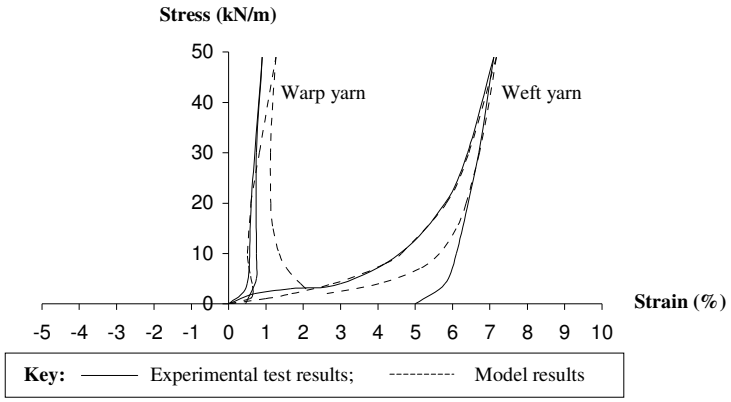


Figure 3: Material and model response for (1:1) stress ratio

## 4. Case Studies

Case studies have been undertaken to assess traditional procedures for the design of TFS. As part of these studies, an investigation has been conducted on how structural curvatures and fabric pattern widths influence the deviation of stress-fields from the theoretical and desired values for the initial equilibrium geometry. Traditional patterning procedures are inherently approximate; therefore a principal aim of the case studies has been to evaluate the structural effect of these approximations.

In these case studies, the behaviour and structural performance of a hyperbolic paraboloid and double ring cone have been analysed, where a stress-field obtained for a quarter model of the latter is shown in Figure 4. All the facets of the developed analysis tool have been brought into play for these case studies.

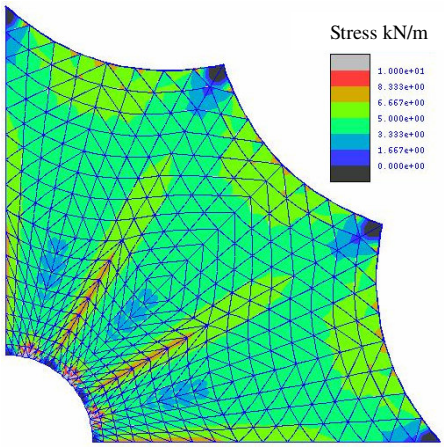


Figure 4: Example of typical stress field for direct stresses

The studies have shown that undesirable stress deviations, as well as shear deformations that are inevitably present, increase with increasing curvature and decrease with the number of fabric patterns. This is as expected and indicates that balanced compromises need to be found for structural curvatures and fabric pattern widths. Indeed, it has been found that although stress-fields vary across the domain of real structures, fabric patterns may be tailored so that stresses may remain permissible (Figure 4). It has also been shown that the integrated design procedure using advanced elements and material modelling is a practical proposition, as sound structures have been arrived at with relatively few iterative adjustments of the cutting patterns and cable lengths. Another significant outcome from the studies is that the integrated design procedure has the potential to result in structures with wider cutting patterns, increasing the buildability of TFS. Finally, the use of accurate and reliable material models for the analysis of TFS has also been shown to be of paramount importance, where it has been found that following the traditional design procedure can lead to undesirable stress fields and wrinkling effects.

## 5. Conclusion

This paper presents a realistic modelling capability for the analysis of TFS, which can form the principal component of an integrated design procedure for such structures. It is considered that the developed analysis tool gives high levels of confidence in the structural analysis of TFS, which is derived through the robustness of the analysis procedure upon which it is based, as well as the accuracy and reliability of the developed finite elements and material model for fabrics. Case studies have been undertaken, which provide an enhanced understanding of the true structural response of TFS, and which have enabled various design issues to be critically considered.

The primary benefit brought by the developed analysis capability is more control and certainty over stress-fields sustained by TFS following erection and under service loads. This leads to the promise of higher quality structures with 'good' stress-fields, as well as neater and cleaner details. It could also provide the necessary functionality for the design of ambitious structures. Other benefits that the proposed analysis capability offers include reduced construction costs, arising from a reduction in the amount of on-site tweaking to reach acceptable forms, and from enabling the use of greater fabric pattern widths without adverse stress-fields.

## References

[1] Abel JF, Haber RB, Salmon DC, Brown ML. Development of computer aided-design of cable-reinforced membrane structures in the U.S.A. *Shells, Membrane and Space Frames, Proceedings IASS Symposium, Osaka*, 1986; **2**: 111-118.

[2] Bradshaw R. Characteristics of fabrics. In *Tensioned Fabric Structures: A Practical Introduction*. Shaeffer RE (ed), ASCE, 1996; Chap 4.

[3] Freeston WD, Platt MM, Schoppee MM. Mechanics of elastic performance of textile materials. *Textile Research Journal*, 1967; **37**: 948–975.

[4] Izzuddin BA. Nonlinear Dynamic Analysis of Framed Structures. PhD thesis, Department of Civil Engineering, Imperial College, University of London, 1991.

[5] Kato S, Yoshino T, Minami H. Formulation of constitutive equations for fabric membranes based on the concept of fabric lattice model. *Engineering Structures*, 1999; **21**: 691-708.

[6] Pargana JB. Realistic Modelling of Tensioned Fabric Structures. PhD Thesis, Department of Civil and Environmental Engineering, Imperial College, University of London, 2004.

[7] Pargana JB, Lloyd Smith D, Izzuddin BA. Advanced material model for coated fabrics used in tensioned fabric structures. *Engineering Structures,* 2007; **29**: 1323-1336.

[8] Phelan DG, Haber RB. An integrated design method for cable-reinforced membrane structures. *Shells, Membrane and Space Frames, Proceedings IASS Symposium, Osaka*, 1986; **2**: 119-126.

Proceedings of the 6th International Conference on
Computation of Shell and Spatial Structures
IASS-IACM 2008: "Spanning Nano to Mega"
28-31 May 2008, Cornell University, Ithaca, NY, USA
John F. ABEL and J. Robert COOKE (eds.)

# Vacuumatics: vacuumatically prestressed (adaptable) structures

Frank HUIJBEN*, Frans van HERWIJNEN

* Eindhoven University of Technology
Department of Architecture, Building and Planning
PO Box 513, 5600 MB Eindhoven, the Netherlands

* ABT Consulting Engineers
PO Box 458, 2600 AL Delft, the Netherlands
e-mail: F.A.A.Huijben@tue.nl

## Abstract

Vacuumatics rely on a relatively "new" and therefore yet unproven structural principle of prestressing incoherent (structural) elements by means of atmospheric pressure, by creating a (partial) vacuum inside an enclosing skin (figure 1). This technique leads to rigid – but reconfigurable – load bearing structures (figure 2), quite analogue to vacuum packed coffee. In an attempt to explore the structural potential of vacuumatically prestressed structures the force distribution throughout a simplistic 2-dimensional representation of such a structure is approached by means of an analytical model. A comparable numerical approach of the technique illustrates a remarkable resemblance in prestress derivation, differentiating a so called "direct" and an "indirect" prestressing component, indicating the significance of the elasticity of the applied skin material. This paper sets out to describe the ongoing study on the structural – as well as geometrical – behaviour of vacuumatics, aiming for a fundamental understanding in and control over the underlying design principles.

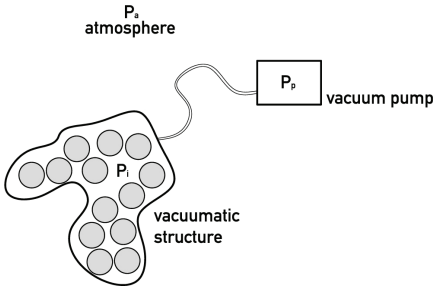


Figure 1: vacuumatics principle

Figure 2: vacuumatically prestressed structure

## 1. Introduction

Vacuumatics can be regarded as a flexible system of foils with enclosed structural (filler) elements that utilises the atmospheric pressure as a rigidifying tool by extracting the air inside this flexible enclosure, hence acting as a compressive force that bonds the individual elements rigidly together and "freezes" the current geometry of the structure. One of the advantages of these types of structures is that the (mostly) incoherent filler elements can be repositioned within their enclosing skin, resulting in the relatively low-tech creation of free-formed structures (Gilbert *et al.* [2]). Furthermore, the ability to control the amount of prestress by simply adjusting the level of vacuum makes it possible for these structures to be reconfigured to new requested shapes, or adapted to required conditions or behaviour (Huijben [3]).

## 2. Vacuumatically prestressing

The atmospheric pressure acting on the enclosing foils causes the skin to be tightly wrapped around the outer surface area of the filler elements, hence creating a structural prestressing of the system. This prestress is not only essential for the structural integrity of vacuumatics (since it effectively joins the filler elements), it also determines the load bearing capacity of the structure as it prevents the filler elements from losing contact in the tensile zone of the structure when externally loaded (figure 3).

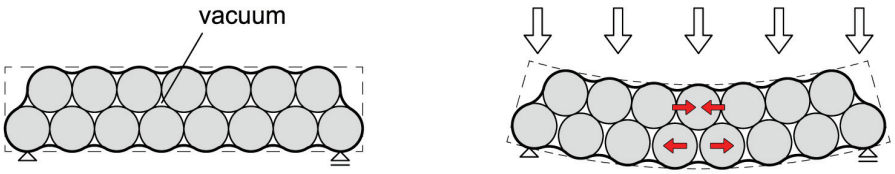


Figure 3: effective structural prestressing

Besides the compressive rigidity of the applied filling material, the elasticity of the skin material in particular is of big influence on the effective amount of prestress. This phenomenon can be best illustrated by a 2-dimensional representation of a vacuumatics structure, consisting out of two circular elements with a certain radius [$R_{el}$], that are enclosed by a flexible skin. In this case, the elasticity of the skin material can be represented by the so called "skin radius" [$R_{sk}$], which describes the curvature of the piece of skin in between the two elements under vacuumatic pressure (figure 4). Theoretically there are two extreme situations: a highly elastic skin material will cover the largest surface area of the filler elements (a), whereas a non-elastic skin will only cover half the elements, hence "spanning" the area in between two elements (c). In reality a sort of intermediate situation will take place (b) since the extremes are physically impossible to occur.

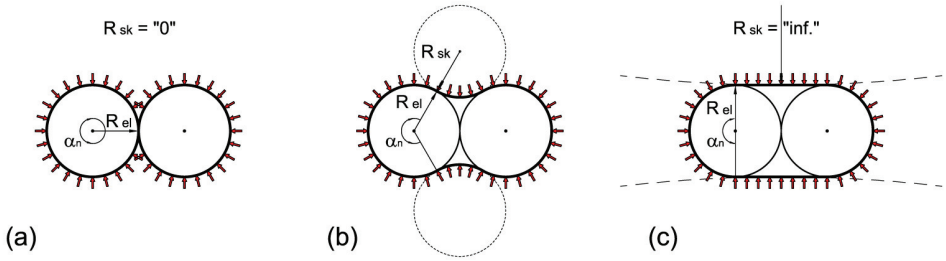


Figure 4: skin radius (related to elasticity of skin material)

## 2.1 Analytical approach

The effective prestressing force acting on each filler element can be divided into two separate components, defined by the so called "covered angle" [$\alpha_n$] which describes the part of the filler element that is covered by a piece of skin (see figure 4). The direct prestressing component is induced by the vacuum pressure acting "directly" on each filler element when the skin is moulded around its surface area (figure 5), whereas the indirect component is induced by the vacuum pressure acting on the piece of skin in between the two filler elements, hence "indirectly" pressing them together (figure 6).

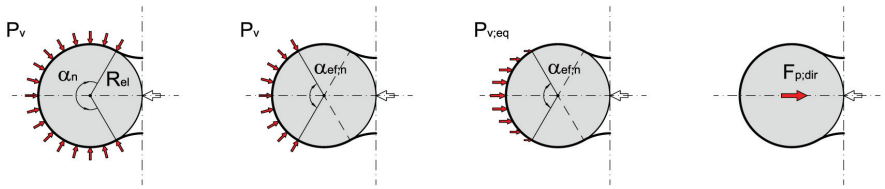


Figure 5: direct prestressing component

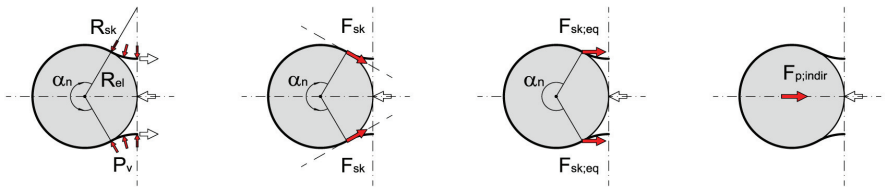


Figure 6: indirect prestressing component

Multi-directional pressure acting on a circular shape can be converted into a non-uniformly distributed parallel load (see figure 5). According to this goniometric behaviour this equivalent load in "axial" direction [$P_{v;eq}$] is larger perpendicular to the surface than it is parallel to the surface, hence explaining the fact that the direct prestressing component will be largest at a covered angle of 180 degrees. The amount of prestress will decrease at larger angles, due to the fact that a part of the pressure is then counteracted by the same pressure in "opposite" direction. The so called "effective covered angle"[$\alpha_{ef;n}$] describes this "reduction" (see figure 5). Analysis of the former led to the following equations for determining the direct and indirect prestressing components, in case of circular shaped filler elements:

$$F_{p;dir} = 2 \cdot R_{el} \cdot P_v \cdot \sin\left(\tfrac{1}{2}\alpha_n\right) \quad (1)$$

$$F_{p;indir} = 2 \cdot R_{sk} \cdot P_v \cdot \sin\left(\tfrac{1}{2}\alpha_n\right) \quad (2)$$

With: $F_{p;dir}$ = direct prestressing component [N], $F_{p;indir}$ = indirect prestressing component [N], $R_{el}$ = radius of filler elements [mm], $R_{sk}$ = skin radius in between filler elements [mm], $P_v$ = vacuum pressure [% atm.], and $\alpha_n$ = covered angle [rad].

Note that both equations (1) and (2) are identical with exception of the value for the radii. Considering the fact that the covered angle [$\alpha_n$] is partially dependent on the elasticity of the skin material, it can be illustrated that the skin radius [$R_{sk}$] largely determines the overall vacuumatic prestressing force [$F_p$] (figure 7). Technically, this prestressing force could therefore have "any" required value, dependent on the elasticity – and strength – of the skin material. Obviously the amount of prestress of vacuumatic structures will also be restricted by several configurational as well as material properties of the filler elements (Huijben *et al.* [4]).

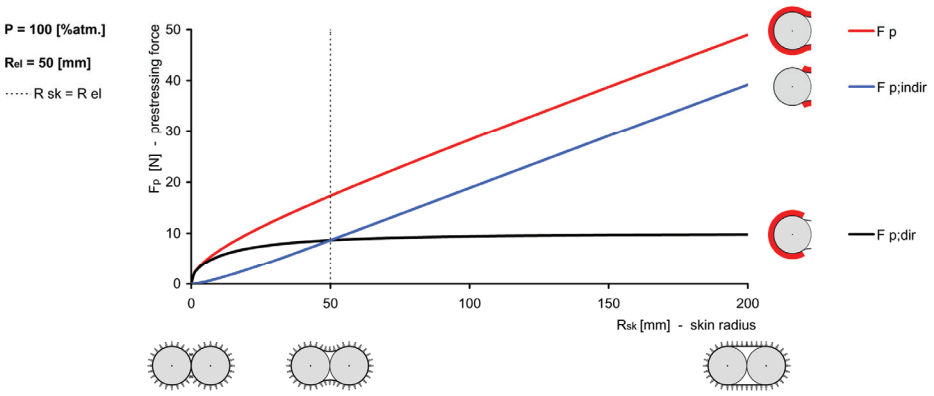


Figure 7: vacuumatic prestressing development (analytical approach)

## 2.2 Numerical approach

In order to compare the analytical results with an equivalent numerical approach, a similar symmetric model is developed, composed out of a tubular shaped rigid body wrapped by a membrane element, both with a relatively small width to simulate a 2-dimensional situation and to reduce the amount of computation data (van Dijk [1]). The vacuum pressure acting on the covering skin is represented by an external pressure load (figure 8).

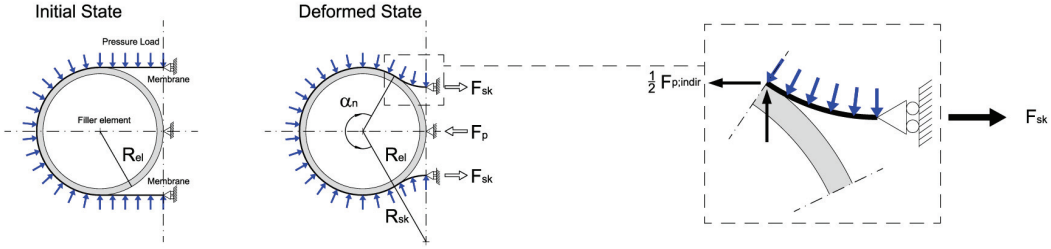


Figure 8: numerical model

The reaction forces along the axis of symmetry describe the horizontal forces that will occur in deformed state, so the centre reaction force [$F_p$] represents the total amount of vacuumatic prestress. The influence of the skin material on the amount of prestress can be derived from the sum of the "upper" and "lower" reaction forces [$F_{sk}$], which (inaccurately) represents the indirect prestressing component like determined with the analytical approach. In this way, however, an horizontal equivalent of the applied pressure acting on the tensioned piece of skin is "ignored", like illustrated in figure 8. By varying the E-modulus of the membrane element, a graphic can be plot, analogue to the one in figure 7, indicating the influence of the elasticity of the skin material on the amount of vacuumatic prestressing force (figure 9). Here, the direct component is derived from the difference between the total prestress and the (inaccurate) "indirect component".

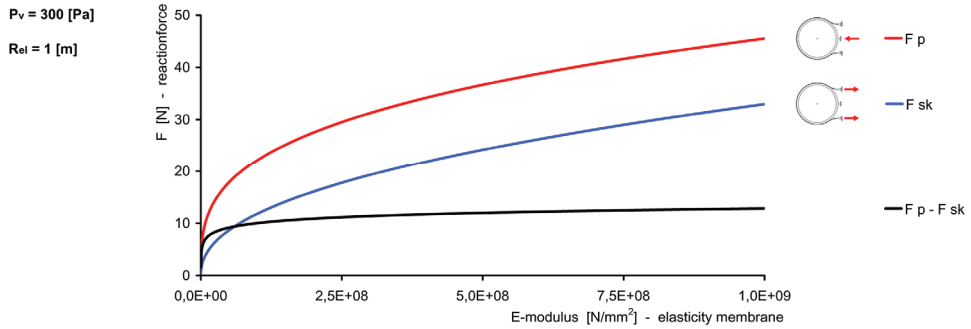


Figure 9: vacuumatic prestressing development (numerical approach)

Remarkable is the resemblance between the two graphics. The slightly different course of the graphic can be attributed to the "ignored" horizontal equivalent pressure acting on the tensioned piece of skin, like explained in figure 8. Higher values of E-modulus of the skin material – and thus a smaller skin deformation – will therefore lead to a closer approximation of the (analytically determined) indirect prestress.

## 3. Conclusion

With vacuumatically prestressed structures the elasticity of the skin material in particular, seems to be one of the controlling factors with respect to the amount of prestress to be achieved. Alternatives to increase the level of vacuumatic prestress might be found in ways like pre-tensioning of the skin in initial state, or post-tensioning of the skin (pneumatic expansion of filler elements) after the vacuum is applied. These issues will be addressed in the next steps of this research as well as the influence of the configurational and material properties of the filler material on the effective amount of vacuumatic prestress.

## References

[1] van Dijk M. Invloed Membraanstijfheid en Wrijving of Voorspankrachten in Vacuümgevormde Membraanconstructies. *Master Research Project*, Eindhoven University of Technology, Eindhoven 2008.

[2] Gilbert J, Patton M, Mullen C, Black S. Vacuumatics. *4th Year Research Project*, Queen's University Department of Architecture and Planning, Belfast 1970.

[3] Huijben F. Vacuumatics, Vacuumatically Prestressed Reconfigurable Architectural Structures. *Graduation Thesis*, Eindhoven University of Technology, Eindhoven 2008.

[4] Huijben F, van Herwijnen F, Lindner G. Vacuumatic Prestressed Flexible Architectural Structures. In *III International Conference on Textile Composites and Inflatable Structures*, Barcelona 2007; 197-200.

Proceedings of the 6th International Conference on
Computation of Shell and Spatial Structures
IASS-IACM 2008: "Spanning Nano to Mega"
28-31 May 2008, Cornell University, Ithaca, NY, USA
John F. ABEL and J. Robert COOKE (eds.)

# Wrinkling evaluation of membrane structures

Lu GUO

Application Engineer, Dr. Eng., Cybernet Systems Co., Ltd.
FUJISOFT Bldg., 3 Kanda-neribeicho, Chiyoda-ku, Tokyo 101-0022, Japan
Email: guolu@cybernet.co.jp

## Abstract

In this paper, wrinkle behavior of membrane structure is studied and evaluated in details. Two wrinkling analysis methods of tensile field theory method and deformation method based on finite element analysis method are compared. The deformation analysis method is suggested to use. Condition, area and reason of wrinkle occurrence are investigated. Structural behavior after wrinkle occurrence is analyzed. Analysis results of deformation, stress distribution and load bearing capability are presented. Energy absorbing behavior of membrane structure is studied from a new view. Positive points of the wrinkle are evaluated. This paper gives some suggests to use the wrinkle effectively in membrane structural design.

## 1. Introduction

Membrane structure construction has recently surged. Membrane material behavior of low compressive strength results in wrinkle occurrence inevitably. The wrinkle often gives a negative image: it is worse, unbeautiful and non-structural. Positive points of wrinkle have not been considered and used enough. In membrane structural design, usually introduce pre-tension stress into membrane surface making structure not occur wrinkle. However, the pre-tension stress is an external factor for membrane material, it can improve material behavior, can't change its behavior basically. And, the pre-tension stress has risk to loss some time. What results would be resulted in by wrinkle have not been studied enough. If assumed membrane structure changes to non-structure after wrinkle occurrence, to understand the non-structural behavior is necessary and interesting. On the other hand, existing other type of membrane structures such as airbag and trampoline etc., their structural function not be influenced by wrinkle occurrence, the wrinkle is positively used to absorb impact energy. A concept of using small stiffness and large deformation material to absorb energy has been applied recently in mechanical engineering and structural engineering. An important idea here is to use native material behavior, not to impose changing it. How to use the concept and the idea to membrane material is one starting point of this research.

Previous study (Guo [1]) has predicted and captured wrinkles of membrane structure successfully. However, the wrinkling evaluation of membrane structure hasn't been done enough. The reasons of wrinkle occurrence and load bearing capability decrease after wrinkle occurrence that haven't been studied clearly.

In this paper, wrinkling behavior of membrane structure is studied in details. Energy absorbing behavior of membrane structure is investigated from a new view. Positive points of the wrinkle are evaluated. This paper gives some suggests to use the wrinkle effectively in membrane structural design.

## 2. Evaluation of wrinkling analysis methods

In wrinkle analysis, the finite element analysis method has been used. According to different assume of wrinkle, two analysis methods can be classified. One is tensile filed theory method. Another one is called to deformation method here, because wrinkle is considered to structural deformation. In this section, the two wrinkling analysis methods by an example are compared. The two analysis methods are evaluated.

### 2.1 Comparison of two wrinkling analysis methods

*2.1.1 Tensile field theory mothod*

Membrane material possesses high tensile strength, but very low compressive strength. The low compressive behavior can result in an inability to support compressive stress, which is usually considered to wrinkle occurrence in the tensile field theory method. Wrinkle evaluation criterrion of principle strain based on the tensile field theory is shown as following equation (1). When element major principle strain $\varepsilon_1$ is larger than zero and element minor principle strain $\varepsilon_2$ is less than or equal to zero, wrinkle occurs. In wrinkling analysis, the compressive element is eliminated.

$$\varepsilon_1 > 0, \varepsilon_2 \le 0 \tag{1}$$

*2.1.2 Deformation method*

Although membrane material possesses small compressive strength, it can bear compressive stress that is considered in the deformation method. Geometrical nonlinear finite element static buckling analysis method and finite element dynamic analysis method both can be used.

*2.1.3 An analysis example*

A analysis example is calculated. Model is a square plane membrane structure. Four coner points are fixed. Finite element dynamic analysis method is used. Concentrated vertical velocity load is acted.

Deformations of two wrinkling analysis methods are shown in figure 2.1. Wrinkle doesn't occur at around edge of concave deformation in figure 2.1a. Wrinkles occur at around edge of concave deformation in figure 2.1b.

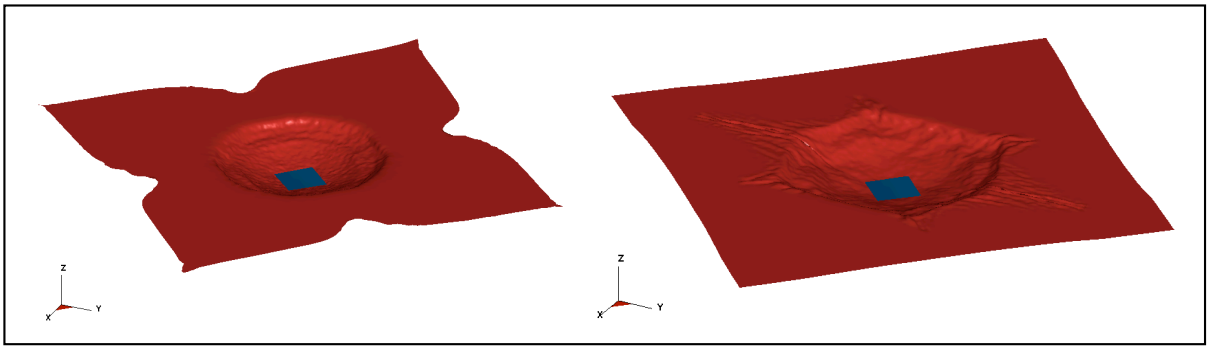

Figure 2.1a: Deformation using tensile field method Figure 2.1b: Deformation using deformation method

### 2.2 Evaluation of wrinkling analysis methods

From the analysis results, following conclusions can be obtained:

- Definition of wrinkle is different in two wrinkling analysis methods.
- Condition, area and reason of wrinkle occurrence can't be understood clearly using tensile field method.
- To study wrinkling behaviour accurately, the deformation method should be used.

## 3. Study and evaluation of wrinkling behavior

To understand what results would be resulted in after wrinkle occurrence that is significant for membrane structural design. In this section, condition, area and reason of wrinkle occurrence are investigated in details. Structural behavior after wrinkle occurrence is analyzed. Analysis results of deformation, stress distribution and load bearing capability are presented. Energy absorbing behavior of membrane structure is studied from a new view. An analysis example is used here. Load is a half sphere shape rigid body.

### 3.1 Deformation and Stress distribution

Figure 3.1 shows deformation of analysis resultes. At step 8, in central area of structure, concave shape defornation happens. Wrinkle doesn't occur. At step 9, at around edge of concave deformation, wrinkles occur long diagonal direction. After step 9, wrinkles continue to increase and extend, but concave deformation extends slowly. The wrinkles restrain the concave deformation extension.

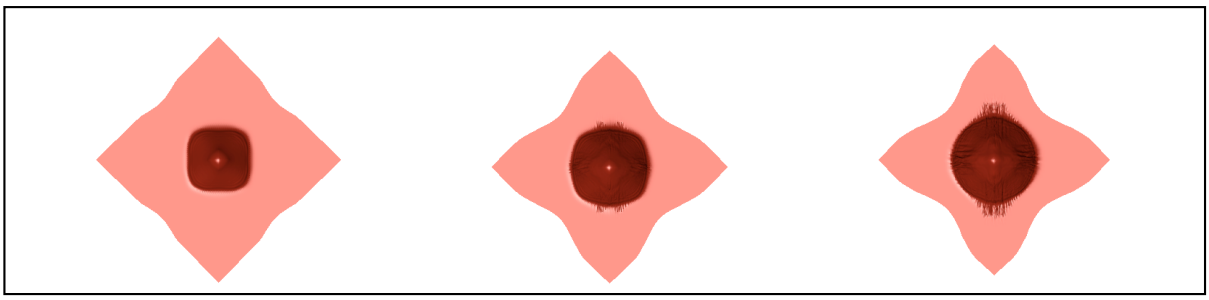

Figure 3.1a: Deformation at step 8 Figure 3.1b: Deformation at step 9 Figure 3.1c: Deformation after step 9

Major principle stress $\sigma_1$ and minor principle stress $\sigma_2$ distributions are shown in figure 3.2. At step 8, at central arer of structure, $\sigma_1$ values of elements are very large (About 500 N/$mm^2$). In interior of concave deformation, $\sigma_2$ values of almost elements are positive. At step 9, at aound central arer of structure, $\sigma_1$ values of elements decrease quickly (About 250 N/$mm^2$). In interior of concave deformation, $\sigma_2$ values of almost elements change to negative. At around edge of concave deformation, $\sigma_2$ values of elements long diagonal direction changes to negative. Form the stress distribution results, the wrinkle occurrence is to release tension stress peak value, prevent membrane material failure. Free boundary allows membrane surface to deform freely that is reason of wrinkles occurring at around edge of concave deformation long diagonal direction.

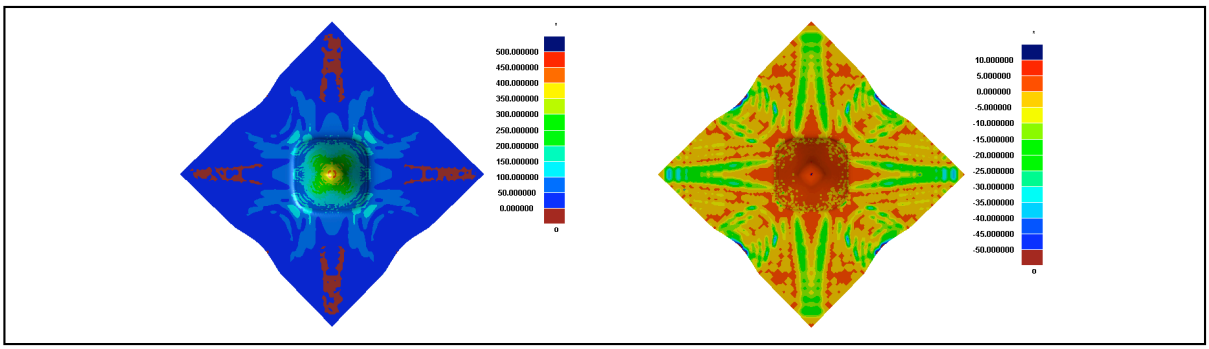


Figure 3.2a: $\sigma_1$ distribution at step 8 Figure 3.2b: $\sigma_2$ distribution at step 8

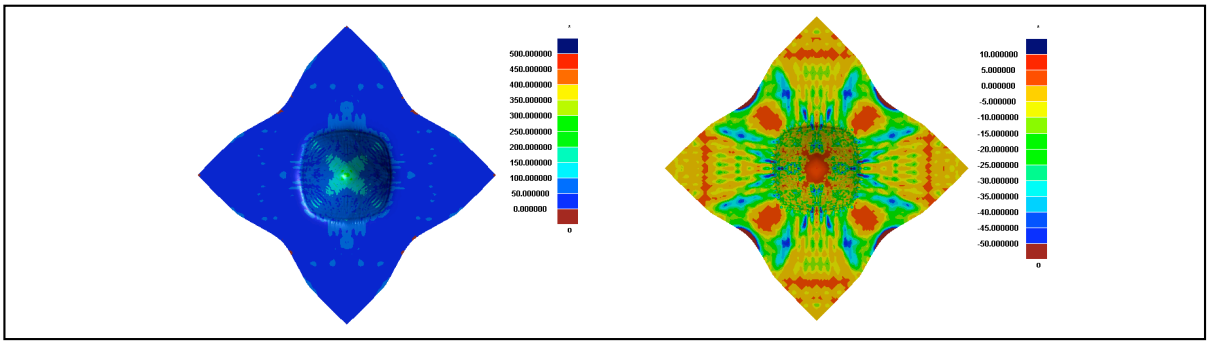


Figure 3.2c: $\sigma_1$ distribution at step 9 Figure 3.2d: $\sigma_2$ distribution at step 9

### 3.2 Load bearing capability

Figure 3.3 shows load bearing capability P curve. At step 9 (Wrinkles occur), P starts decreasing. After step 9, P keeps decreasing. The load bearing capability decreases after wrinkle occurrence. In interior of concave deformation, wrinkles occur too, and increase gradually. Contact force between load rigid body and membrane surface decreases gradually that is the reason of the load bearing capability decrease.

### 3.3 Energy absorbing behavior

To understand whether membrane structure changes to non-structure after wrinkle occurrence, energy absorbing behavior is studied. Figure 3.4 shows internal energy absorbing curve. At step 9, curve gradient starts increasing. The wrinkles occurred on membrane surface continue to absorb energy. After wrinkle occurrence, load bearing capability decreases, however, energy absorbing of wrinkles increases. It can be considered to its structural function still works.

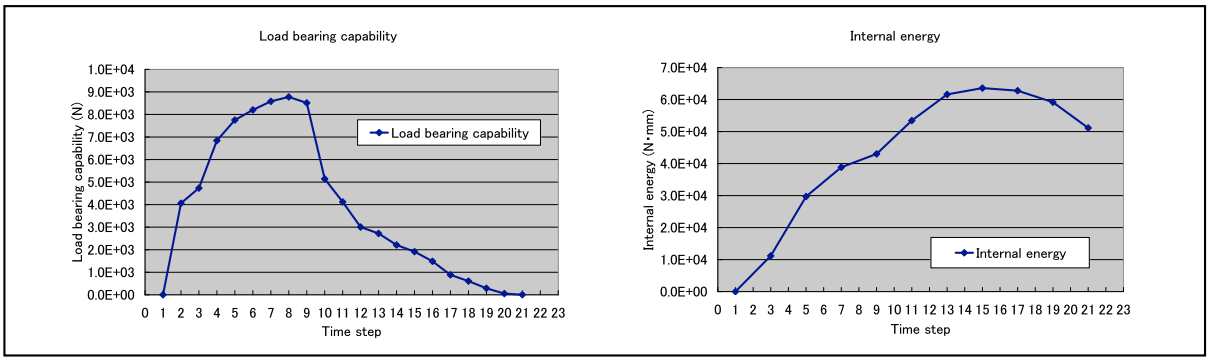


Figure 3.3: Load bearing capability

Figure 3.4: Energy absorbing

## 4. Effective use of wrinkle

The wrinkle can be seen from positive view, and can be used effectively in membrane structural design. In this section, the positive points of wrinkle are evaluated. Some suggests are given in membrane structural design.

### 4.1 Evaluation of wrinkle

From the analysis results, the wrinkle shows some positive points. One is wrinkles release tension stress peak value to prevent membrane material failure. Another one is that wrinkles absorb large energy.

### 4.2 Some suggests in membrane structural design

In membrane structural design, it is better to design free boundary for preventing membrane surface failure. Use positively the fine impact energy absorbing behavior of membrane structure by wrinkle deformation that can avoid other structure or other partial structure not suffering excess influence under crash load.

## 5. Conclusions

The winkling analysis and evaluation have been presented. The following conclusions can be drawn based on the results.

- When high tension stress is needed to release, wrinkles occur.
- After wrinkle occurrence, load bearing capability decreases, energy absorbing increases.
- Wrinkles can prevent membrane material failure and absorb large internal energy.

## References

[1] Guo L. Wrinkle analysis of membrane structures due to out-of-plane loading by using LS-DYNA. *Shell and Spatial Structures: Structural Architecture – Towards to the Future Looking to the Past*, Majowiecki M (ed). Academic Press: Venice, 2007; 157-158.

Proceedings of the 6th International Conference on
Computation of Shell and Spatial Structures
IASS-IACM 2008: “Spanning Nano to Mega”
28-31 May 2008, Cornell University, Ithaca, NY, USA
John F. ABEL and J. Robert COOKE (eds.)

# Wrinkling of stretched elastic films via bifurcation

Ron-Bin CHENG* & Tim HEALEY

Department of Theoretical & Applied Mechanics
Cornell University
*rc284@cornell.edu

**Abstract**

Consider a thin rectangular elastic sheet or film. The formation of transverse wrinkles is typically observed while clamping two opposite ends and stretching in that direction. We adopt a Föppl - von Kármán model for the film, and study the problem via numerical bifurcation theory. Note that the primary planar solution is not homogeneous, due to the realistic boundary conditions (no lateral contraction is allowed at the clamped boundaries). As such, even the family of planar solutions must be computed numerically; we then seek non-planar bifurcating solutions. In particular, there are two natural continuation parameters appearing in our problem: (1) the gross or nominal stretch ratio; (2) the reciprocal of the square of the thickness (the ratio of the in-plane stiffness to the bending stiffness). We follow non-planar equilibria via numerical path-following techniques. Switching back and forth between the two continuation parameters allows us to trace the bifurcating solution branches in the regimes of interest, viz., where the continuation parameter is very “large” (corresponding to “very thin” sheets). We then pinpoint stable wrinkled patterns, corresponding to bifurcated non-planar solutions that render the potential energy a local minimum.

Proceedings of the 6th International Conference on
Computation of Shell and Spatial Structures
IASS-IACM 2008: "Spanning Nano to Mega"
28-31 May 2008, Cornell University, Ithaca, NY, USA
John F. ABEL and J. Robert COOKE (eds.)

# A comparison of four flattening methods for tensioned fabric structures

Slade GELLIN*

*Buffalo State College
Buffalo, NY 14222 US
gellins@buffalostate.edu

## Abstract

A comparison of four flattening methods is made for a representative template region for a tensioned fabric membrane structure. The flattening methods are incorporated into the proprietary patterning software of a major manufacturer of these structures. The author is the principal programmer for this software.

## 1. Introduction

The patterning of tensioned fabric structures has been studied for a long time, particularly since the development of computer simulation software for such structures. These methods, referred to herein as flattening methods, seek to find a 2D shape, referred to herein as a(n uncompensated) template, within the constraints of fabric roll width that best approximates a portion of a 3D membrane surface, referred to herein as the shaped model. What is considered "best" for a given template depends on what analytical tools are available, the manufacturing philosophy of the company making the templates, and the details of how the templates are connected to each other, cables, and fixed supports.

The flattening methods can generally be divided into two classes (Moncrieff and Topping [4]), referred to herein as structural flattening and geometric flattening. Structural flattening methods will take the region of the shaped model under consideration for a template, and performs a structural analysis on this region where displacements at each node have been specified to force the region into a plane. The structure is free to deform within the plane, and is supported against rigid body motion in the plane in a statically determinate manner. Proponents of this methodology rightly claim that the error in flattening is spread out over the template, and that output stresses of the analysis can be used as an additional criterion on the feasibility of the template.

Geometric flattening methods will take a region of the model and super-impose a discretized perimeter consisting of interconnected points, referred to herein as template points. Lines across the region, referred to herein as web lines, connect these template points. The number of web lines equals the number of template points minus 3; that is, when looking in "plan view", the perimeter together with the web lines appears as a pattern suitable for statically determinate 2D truss analysis. It is well documented that this arrangement can be "unfolded" without additional strain to a 2D shape. Proponents of this methodology are most concerned with geometric properties of the template, particularly the perimeter, which, unlike with structural flattening methods, is generally conserved in the unfolding process.

Regardless of flattening method, the template then undergoes the same processes and is subject to the same concerns. The template must be compensated; the edges are modified to account for connections to other templates, cables or fixed boundaries; and, ideally, has efficient fabric utilization.

The author has been involved in development and implementation of a computer program that contains a comprehensive patterning system for a world-wide manufacturer of tensioned fabric structures and its subsidiaries. The philosophy of this program (Gellin [2, 3]) is that the engineer should make one model adequate for engineering analysis, with a finite element mesh sufficient for patterning, *without regard for the details of patterning*. The pattern designer will draw seam lines super-imposed upon the shaped model which

are reflective of template regions and manufacturing details at cable and steel connection points. Thus, these seam lines are not necessarily along membrane element edges. Algorithms, not described in this extended abstract, can be used to modify seam lines in order to maximize fabric utilization, thus eliminating the need for iterative model adjustments by the engineer.

The program allows the user to choose from 4 flattening methods, two of which are geometric and two of which are structural in nature. The geometric methods were developed first, because the subsidiary company for which the author was working used those methods. Specifically, the method used, referred to herein as the chord method, took a region of the model containing an integral number of membrane elements, surrounded it with a perimeter, and, using the intervening node points as template points, drew straight line webs, and unfolded the template. Though the perimeter was conserved, errors in the fill direction were estimated and in the warp direction never examined. The second geometric method developed for the program, referred to herein as the surface method, constructed the same type of web arrangement (though using the designer developed seam lines and segmentation choices), but these web lines had lengths that were geodesic distances from point to point. When flattened, the straight line distance between the two end points of a web line in the flattened template matched the geodesic distance between those points in the shaped model. Generally, for a "longer" template, this removed the geometric error in the fill direction.

The program allows the user to check other point-to-point distances within the template, comparing the straight line distance in the flattened template to the corresponding geodesic line in the shaped model. Using these checks, the size of the warp error was discovered to be alarming large for both chord and surface methods of flattening. An algorithm, not described in this extended abstract, was developed to incorporate the unfolding method with constraints. These constraints introduced error elsewhere in the template, which can be partially controlled by additional constraints. The method allows the designer to choose which geometric quantities are most important to his company for the manufacture and installation of template fabric structures.

Subsequent to the development of the geometric methods, a request of one of the subsidiary companies resulted in the incorporation of a structural method of flattening in the program. Since seam lines were not confined to membrane element edges, a method, referred to herein as the minimum energy method, was developed where a membrane region was chosen to enclose the template region; this membrane region underwent the structural procedure described above; and, then, the template points were mapped in this flattened region using a method consistent with the finite element analysis, and then interpolated together to form the template outline.

Most recently, the parent company requested that the region developed for a template be re-meshed, re-shaped, and then flattened using the new mesh. This method is referred to herein as the minimum energy method with re-shaping.

Another structural method has attracted the author's attention (Bletzinger *et al.* [1]) whereby the coordinates of a flattened template are modified to minimize the stress deviation from the ideal pre-stress over the shaped model after re-assembly of the templates. Several conceptual details of that method need to be worked out before incorporation into the program could take place, should that be the corporate decision.

In this extended abstract, a test case is developed and flattened using each of the four incorporated methods. Where applicable, various measures are used to compare the results. Depending on the needs of the template and the structure within which that template will be installed, the engineer can then make a decision as to which method is best.

## 2. Test Case and Results

Figure 1 depicts the test case. The shaped model is a symmetric "hy-par" structure, with planar expanse of 20 ft and with the x-axis end points 10 ft below the y-axis end points. The template outline is shown in the center of the figure and consists of four geodesics. The template is segmented with 6 segments in the vertical (fill) direction and 10 segments in the horizontal (warp) direction. Five checks approximately parallel to warp and nine checks approximately parallel to fill will be made.

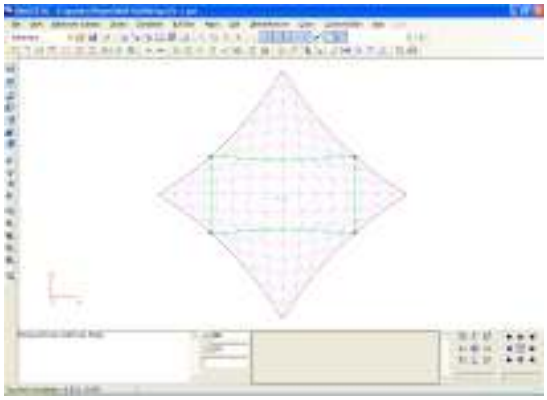

Figure 1: Shaped model and template

Six cases will be examined. For Case 1, the template will be flattened using the chord method. This is the method used by one of the subsidiary companies until about 2000. Figure 2 displays the flattened template indicating the web lines and the check lines. For Case 2, the template will be flattened using the surface method. Case 2A is the same as Case 2, except the warp checks will be changed to constraints. This is typical of the method used by the subsidiary company today. Case 2B is the same as Case 2A, except the outermost fill check line is changed to a constraint. This, again, is something the subsidiary company would do in this particular template. For Case 3, the template will be flattened using the minimum energy method with an enclosing subset. Figure 3 displays the template and its subset. For Case 4, the template will be re-meshed, re-shaped, and then flattened using the minimum energy method.

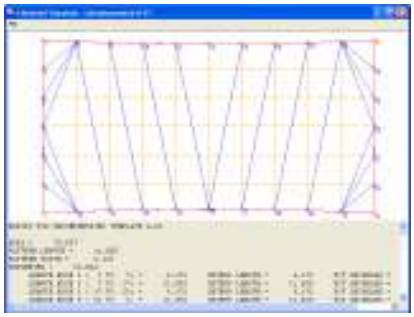

Figure 2: Flattened template results for Case 1

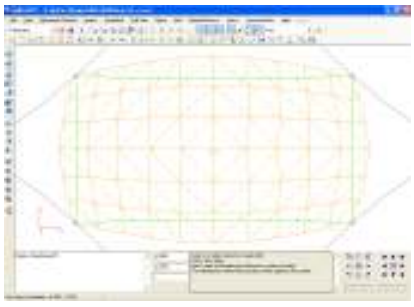

Figure 3: Subset associated with template for Case 3

Results for the comparative study are shown in Figure 4. The geometric flattening cases (1, 2, 2A, 2B) all yield exact results for the edge lengths by design. Case 2 will yield exact results for the fill checks. Cases 2A and 2B will yield exact results for those distances that have been chosen to be constrained. The structural flattening cases (3, 4), while not satisfying any of the measurements exactly, yield overall excellent results. While the re-

meshing technique of Case 4 may have some debatable issues, that is, its true relationship to the shaped model supplied by the engineer, it appears to be somewhat superior to Case 3. It is also the only case where the template area prior to flattening is readily available (70.268 $ft^2$).

| Case | Area ($ft^2$) | Edge Length, Warp (ft) | Edge Length, Fill (ft) | Error, Central Warp Check (%) | Error, Outermost Fill Check (%) | Error, Central Fill Check (%) |
|---|---|---|---|---|---|---|
| 1 | 70.657 | 11.830 | 6.172 | 1.470 | -0.384 | -0.439 |
| 2 | 70.765 | 11.830 | 6.172 | 1.044 | 0 | 0 |
| 2A | 70.398 | 11.830 | 6.172 | 0 | 0.692 | -0.010 |
| 2B | 70.293 | 11.830 | 6.172 | 0 | 0 | -0.040 |
| 3 | 70.331 | 11.831 | 6.157 | 0.178 | -0.087 | -0.064 |
| 4 | 70.267 | 11.792 | 6.161 | 0.204 | -0.022 | -0.062 |

Figure 4: Results

Cases 3 and 4 provide stress data as part of their output. For each stress, the range in Case 3 encompasses that of Case 4. This is not surprising, since the area flattened in Case 3 encloses that of Case 4.

It is believed that different engineers looking at Figure 4 will draw different conclusions. It is the opinion of the author that Case 2B is certainly adequate for patterning when geometry is most important. The warp check error in Cases 3 and 4 may be large enough compared to the warp compensation of some fabrics to give engineers using structural methods of flattening pause for concern; of course, the stress output can be examined to see if there really is a problem. On the other hand, the lack of stress data in Case 2B, as well as other geometric flattening method cases, leaves an element of doubt concerning possible tear or wrinkle areas developing upon installation, particularly in the template corners. Ironically, Case 1, despite its demonstrated flaws, has been the method of choice for a variety of successful structures worldwide.

## Acknowledgement

The author would like to thank Taiyo-Kogyo Corporation, and its US subsidiary, Birdair, Inc., for their support of this research.

## References

[1] Bletzinger KU, Linhard J, Wuchner R. Recent advances and generalized aspects of numerical form finding and patterning methods. *Proceedings of the IASS Conference, Venice, Italy* 2007.

[2] Gellin S. Patterning for tension fabric structures. *Proceedings of the 5th International Conference on Engineering Design and Automation, Las Vegas, Nevada* 2001, pp 482-487.

[3] Gellin S. Improvements in patterning for tension fabric structures. *Proceedings of the 6th International Conference on Engineering Design and Automation, Maui, Hawaii* 2002, pp. 215-218

[4] Moncrieff E and Topping BHV. Computer methods for the generation of membrane cutting patterns. *Computers and Structures* 1990; **37**:441 – 450.

Proceedings of the 6th International Conference on
Computation of Shell and Spatial Structures
IASS-IACM 2008: “Spanning Nano to Mega”
28-31 May 2008, Cornell University, Ithaca, NY, USA
John F. ABEL and J. Robert COOKE (eds.)

# On the calculation of elastic systems having blocks and sagging cables

Vadym GORDEIEV*, Oleksandr OGLOBLYA, Maryna SHYMANOVSKA

*Vice Chairman of OJSC "V.Shimanovsky UkrRDIsteelconstruction", Member of IASS.
1, Vyzvolyteliv prospect, Kyiv, 02660, UKRAINE. E-mail: gor@urdisc.com.ua

## Abstract

The non-linear systems under deformation, incorporating long sagging cables, which have been passed through running and fixed blocks, are analyzed in the paper. The considerable displacements of the elements in the system and remarkable deformations of cables are taken into consideration.

The systems of similar types were highlighted in scientific works (Gordeiev, Shymanovska [1], [2], [3]). In these reference works the portions of cables between the nodes are supposed as to be rectilinear. In this paper such supposition is absent. The cables may be sagged under the action of load due to dead weight or due to any other load, distributed uniformly along the cable length. The exact solution for strongly extended cable, fastened by its ends not known in scientific references was obtained and shown.

Some examples of such systems are aerial nets of long-wave, medium-wave and short-wave radio broadcasting stations, which are supplied with running and fixed blocks and other mechanisms for convenience of erection and which make it possible to raise and lower the net repeatedly. Into the composition of net may be entered a pliable elements made of synthetic materials or spiral-type twisted wires similar to the handset cord.

## 1. Design diagram

As the basis of design diagram may be regarded the sagging cables under tension, linked together with imaginatory nodal insertion pieces. This nodal insertion piece is a solid body of vanishingly small dimensions supplied with lifting eyes for passage of the cables. The cables are able to slop inside them without friction. Besides, in design diagram there are present the braces of two types. The first type of the brace is an arrangement, which prevents to displacement of nodal insertion piece in the space following by one direction. The second type of the brace may be considered as an arrangement, hindering displacement of the cable through the lifting eye.

Let’s assume that at each cable a zero pint and positive direction is selected. Then in the non-strained condition the scale is marked off on the cable for determination of angular coordination per unit length. In such a case the position of nodal insertion piece will be characterized by three coordinates in the space: $x_1$, $x_2$, $x_3$ so, if this insertion piece pass $k$ cables, then in addition to $k$ coordinates $s_1,\ldots,s_k$., that is the nodal insertion piece under consideration has $k + 3$ degrees of freedom.

The concentrated forces may effect on the insertion piece. On each cable may act load, uniformly distributed along its unstrained length and having fixed direction.

## 2. The relationships for cable portion

Let’s consider the cable portion having tensional rigidity $G$ located between adjacent nodal insertion pieces and perceiving load due to own weight of intensity $\gamma$ = const. The nodal joint which corresponds to the lesser meaning of angular coordinate on the cable we will call as initial and the second one as final. Let the coordinates of the initial nodal joint will be – $s^b$, $x^b{}_1$, $x^b{}_2$, $x^b{}_3$, the final one – $s^e$, $x^e{}_1$, $x^e{}_2$, $x^e{}_3$ having in mind that by letter $s$ is indicated the angular coordinate on the cable, by letter –Cartesian coordinates in the space. In addition, by index $b$ are marked the initial nodal joint coordinated and by index $e$ the coordinates of the final

nodal joint correspondingly. .Let's suppose that the load acting on the cable has components along coordinate axes $\gamma_1$, $\gamma_2$, $\gamma_3$.

To obtain the design relationships we are able to use the principle of minimum potential energy. The potential energy of the cable portion in the state under consideration is expressed by functional:

$$\Pi = \int_{s^b}^{s^e} \left( \frac{\varepsilon^2}{2} G - \sum_{i=1}^{3} x_i \gamma_i \right) ds + \Pi_0 ; \; \varepsilon = \sqrt{\sum_{i=1}^{3} \left( \frac{dx_i}{ds} \right)^2} - 1; \qquad (1)$$

where $\Pi_0$ - constant, depending on the initial condition of the cable.

The functions $x_i$; ($i$ = 1,2,3) of coordinate $s$, featuring equilibrium position of the cable and serving as extremals of functional ( 1 ), should meet the Euler's system of differential equations for this particular functional:

$$\frac{d}{ds}\left( \frac{\varepsilon}{\varepsilon + 1} \cdot \frac{dx_i}{ds} \right) + \frac{\gamma_i}{G} = 0 \quad (i = 1,2,3); \qquad (2)$$

as well as to boundary conditions:

$$\text{when } s = s^b \qquad x_i = x^b{}_i; \quad \text{when } s = s^e \qquad x_i = x^e{}_i \quad (i = 1,2,3). \qquad (3)$$

By substitution in equation ( 2 ) and ( 3 ) it is possible to be convinced that the exact solution of the problem may be represented by functions:

$$x_i = x_i^{md} + m\left[ \frac{l_i}{l} \left( \operatorname{asinh}\sigma + \frac{\gamma m}{G}\sigma - \varsigma^{md} \right) - \frac{\gamma_i}{\gamma} \left( \sqrt{1+\sigma^2} + \frac{\gamma m}{G} \cdot \frac{\sigma^2}{2} - \eta^{md} \right) \right] \quad (i = 1,2,3). \qquad (4)$$

$$\left.\begin{array}{l} x_i^{md} = \dfrac{x_i^b + x_i^e}{2}; \;\; l_i = x_i^e - x_i^b + h\dfrac{\gamma_i}{\gamma} \quad (i = 1,2,3); \; h = -\displaystyle\sum_{i=1}^{3} \frac{\gamma_i}{\gamma}\left( x_i^e - x_i^b \right) \;\; l = \sqrt{\sum_{i=1}^{3} l_i^2}; \;\; S = s^e - s^b; \\ \mu = \dfrac{h}{s}; \;\; \lambda = \dfrac{l}{s}; \;\; \nu = \dfrac{\gamma S}{2G}; \;\; \varsigma^{md} = \operatorname{atanh}\dfrac{\mu p}{p+\nu} + \dfrac{\mu\nu}{p+\nu}; \; \eta^{md} = \dfrac{S}{2m}\left[ \dfrac{1}{p} + \dfrac{\nu}{2}\left( \dfrac{\mu}{p+\nu} \right)^2 + \dfrac{\nu}{2} \right]; \\ m = \dfrac{l}{2(\beta+\nu)}; \; \beta = \operatorname{atanh} p; \; \sigma = \dfrac{\beta+\nu}{\lambda}\left( \dfrac{2s}{S} + \dfrac{\mu}{p+\nu} - \dfrac{s^e + s^b}{S} \right). \end{array}\right\} \qquad (5)$$

The parameter $p$, appearing in the formulae given above is the single positive root of transcendental equation

$$\left( \frac{\lambda}{\operatorname{atanh} p + \nu} \right)^2 \cdot \frac{1}{1 - p^2} + \left( \frac{\mu}{p+\nu} \right)^2 = \frac{1}{p^2}. \qquad (6)$$

The root is located within interval $0<p<1$ and is determined by numerical method.

By substitution of relationship ( 4 ) into ( 1 ), after transformation we may obtain

$$\varepsilon = \frac{\gamma m}{G}\sqrt{1+\sigma^2}; \qquad (7)$$

$$\Pi = \frac{\gamma S}{2}\left( \frac{\mu^2}{2(p+\nu)} - \frac{1}{2p} - \frac{\nu}{6} + \frac{\lambda^2}{2(\beta+\nu)} - \mu\frac{s^e + s^b}{s} \right) + \Pi_0. \qquad (8)$$

The force in the cable is defined with application of the formula ( 7 ):

$$\hat{O} = \gamma m\sqrt{1+\sigma^2}. \qquad (9)$$

In such a manner if coordinates of nodal insertion pieces positioned at the ends of the cable portions are known, the displacements and forces in any point of the cable can be determined by exact relationships ( 4 ) and ( 9 ) in the capacity of the function of angular coordinate *s*. In such a case the displacements and relative elongations of the cable may be of any amount.

## 3. The principle for calculation of the system

The energy connected with the cable portion and positioned between two adjacent insertion pieces is given by expression ( 8 ). It involves both the elastic energy and energy of load, acting on the cable. Besides, the design diagram envisages a probability to apply loads to the nodal insertion pieces. Naturally these loads will contribute to energy of the system. Therefore, concentrated force applied to nodal insertion piece and having projections on coordinate axes $Q_1$, $Q_2$, $Q_3$, will add to potential energy of the system the following value

$$\Pi_j = -\sum_{i=1}^{3} Q_i x_i + \Pi_{j_0} \; ; \qquad (10)$$

where $\Pi_{j_0}$ - constant, determined by the initial position of the joint.

If it is possible to add the energy of cable portions and nodal loads we can obtain the expression for complete energy of the system , depending upon spatial and angular coordinates of all nodal insertion pieces as well as on parameters *p*, involved into equation of the type ( 6 ), by one for every cable portion.

The spatial and angular coordinates are subjected to determination, if these coordinates weren't fixed by braces. Such unknown values may be defined proceeding from conditions of steady-state characteristics of potential energy of the system. The conditions are obtained by means of differentiation of the expression for potential energy of the system according to unknown coordinates and by making equal the expressions for zero derivative Hence, a necessary number of equations may be compiled. The second group is formed by equations of the type ( 6 ), number of which is equal to number of unknown parameters *p*. All equations appeared to be as non-linear and transcendental.

The system of equations may be obtained by another way, by substitution of summation and differentiation order, as it is usually done with the use of finite elements method. By means of differentiation for potential energy of the cable portion according to unknown coordinates we obtain the following:

$$\left.\begin{aligned}
&\frac{\partial \Pi}{\partial s^b} = \frac{\gamma S}{2}\left(\frac{1}{\rho} - \mu + \frac{\nu}{2} + \frac{\nu\mu^2}{2(\rho+\nu)^2} + \frac{\nu\lambda^2}{2(\beta+\nu)^2}\right); \frac{\partial \Pi}{\partial x_i{}^b} = \frac{\gamma S}{2}\left(\frac{\gamma_i}{\gamma}\cdot\frac{\mu}{\rho+\nu} - 1 - \frac{l_i}{l}\cdot\frac{\lambda}{\beta+\nu}\right) \quad (i = 1,2,3) \\
&\frac{\partial \Pi}{\partial s^e} = -\frac{\gamma S}{2}\left(\frac{1}{\rho} + \mu + \frac{\nu}{2} + \frac{\nu\mu^2}{2(\rho+\nu)^2} + \frac{\nu\lambda^2}{2(\beta+\nu)^2}\right); \frac{\partial \Pi}{\partial x_i{}^e} = -\frac{\gamma S}{2}\left(\frac{\gamma_i}{\gamma}\cdot\frac{\mu}{\rho+\nu} + 1 - \frac{l_i}{l}\cdot\frac{\lambda}{\beta+\nu}\right) (i = 1,2,3)
\end{aligned}\right\} \qquad (11)$$

The derivatives due to potential energy of the nodal loads ( 10 ) according to spatial coordinates of nodal insertion pieces have the following view:

$$\frac{\partial \Pi_j}{\partial x_i} = -Q_i \, . \qquad (12)$$

By summation of derivatives ( 11 ) and ( 12 ), taken by the same coordinate and by making equal this amount to zero, we are able to obtain all desired equilibrium equations.

The computation methods are considerably easier to compose, if not to be based on idea of equilibrium equations solution, but using the idea aimed at minimization of potential energy of the system. The coordinates of potential energy minimum point in the space of unknowns comply with such meanings of unknowns, whereby the system is under condition of stable equilibrium. The unknowns are displacements of nodal insertion pieces in our particular case in succession.

The potential energy of the system may be treated as smooth function, having in each point of the space in the coordinates of nodal insertion pieces the first and the second partial derivatives. This provides a way for

approximation of potential energy of quadric functions, on the basis of the energy meanings itself, using the first and the second partial derivatives in one point:

$$\Pi = \frac{1}{2}\sum_{i=1}^{n}\sum_{j=1}^{n}\left.\frac{\partial^2\Pi}{\partial x_i \partial x_j}\right|_0 \left(x_i - x_i^0\right)\left(x_j - x_j^0\right) + \sum_{i=1}^{n}\left.\frac{\partial\Pi}{\partial x_i}\right|_0 \left(x_i - x_i^0\right) + \Pi\big|_0 \; ; \qquad (13)$$

where $n$ - dimensionality of the space in which the function $\Pi$;
$x_1,\ldots,x_n$ – coordinates of minimum of the function under approximation;
$x^0{}_1,\ldots,x^0{}_n$ – coordinates of 0 point.

The vertical line with index 0 implies, that meanings of function is calculated at the point 0.

The detection of coordinates of quadric function minimum is performed through the use of solution of linear algebraic equations:

$$\sum_{j=1}^{n}\left.\frac{\partial^2\Pi}{\partial x_i \partial x_j}\right|_0 \left(x_j - x_j^0\right) + \left.\frac{\partial\Pi}{\partial x_i}\right|_0 = 0 \qquad (i = 1,\ldots,n). \qquad (14)$$

So. is rather simple to find coordinates of approximating function minimum. The natural successive approximation method where the point for the next in turn approximation may serve the point of quadric function minimum, taken from previous approximation is called as Newton's method. This method is characterized by quick quadric convergence in the vicinity of solution, but far away from the point of solution it may be diverged or lead to incorrect result. The main disadvantages of Newton's method may be eliminated, when quadric approximation function is used only for determination of line of inquiry. At the same time an investigation is carried out as one-dimensional by numerical method application. This Newton's method modification is recommended for the use at initial stage of the problem solution. The ordinary Newton's method is preferable at the final stage.

## 4. Recommendations aimed at realization of the calculation method

The system of linear algebraic equations ( 14 ) composed and solved at every iteration is a complete analogue of the system of equations with the use of finite elements method. If the structure under review presents itself something more complicated than the spatial cable system and incorporates both bar-shaped or either other finite elements, so for such elements it is necessary to write down the formulae used for finite elements method. Then there is a need to accumulate the coefficients of the equations system ( 14 ), taking into consideration a contribution from each finite element successively.

Every iteration process, while calculating non-linear system under deformation is similar to calculation of some non-linear system under deformation also. Such iteration will be repeated till the moment when the required accuracy of solution is to be reached. The form of sagging and forces of individual cables are not subjected to calculation. It is sufficient to do such operation after completion of iteration process. As regards a determination of the parameter $p$, it should be noted that its meaning must be defined at every iteration process for each cable portion during solution of the equation ( 6 ).

Naturally, only some recommendations have been given here, which make easier to provide an algorithmic presentation of the problem to be sought.

## References

[1] Gordeev VN., Shimanovskaya MA. Statics of nonlinear elastic cable-stayed systems with slipping flexible cables. *International Applied Mechanics*, New York, 2006; – **42**: 560–567.

[2] Gordeiev V., Shymanovska M. Analysis of spatial nets allowing for slippery ropes. In *Proceedings of the International Symposium on Shell and Spatial Structures*. – V1. – Bucharest, Poiana Brasov (Romania), 2005; 161–168.

[3] Gordeiev V., Shymanovska M. Shaping properties of nets with slipping cables. In *Proceedings of the joint CIB, Tensinet, International Conference on Adaptability in Design and Construction*. Eindhoven University of Technology, V 2. The Netherland, 2006; 218–222.